Carbohydrate Polymers 115 (2015) 373–378

Contents lists available at ScienceDirect

Carbohydrate Polymers

journal homepage: www.elsevier.com/locate/carbpol

Compare study cellulose/Mn_3O_4 composites using four types of alkalis by sonochemistry method

Lian-Hua Fu[a,1], Shu-Ming Li[b,1], Jing Bian[a], Ming-Guo Ma[a,*], Xing-Luan Long[a], Xue-Ming Zhang[a], Shi-Jie Liu[c]

[a] Beijing Key Laboratory of Lignocellulosic Chemistry, College of Materials Science and Technology, Beijing Forestry University, Beijing 100083, PR China
[b] School of Chemical Engineering and Technology, Tianjin University, Tianjin 300072, PR China
[c] State University of New York, College of Environmental Science and Forestry, Syracuse, NY 13210, USA

ARTICLE INFO

Article history:
Received 11 July 2014
Received in revised form 14 August 2014
Accepted 19 August 2014
Available online 8 September 2014

Keywords:
Cellulose
Mn_3O_4
Composites
Sonochemistry
Alkalis

ABSTRACT

The purpose of this article was to explore the influences of alkalis types on the cellulose/Mn_3O_4 composites via a sonochemistry method. In this study, cellulose/Mn_3O_4 composites were successfully fabricated using four types of alkalis (urea ($CO(NH_2)_2$), hexamethylenetetramine ($(CH_2)_6N_4$, HMT), NaOH, and KOH) by an environmentally-friendly sonochemistry method. The phase, shape, thermal stability, and the formation mechanism of the cellulose composites were researched in detail. Experimental results demonstrated that the types of alkalis played an important role in the phase, shape, dispersion, and thermal stability of cellulose/Mn_3O_4 composites. By thermal treatment of cellulose/Mn_3O_4 composites at 600 °C for 3 h in air, the Mn_3O_4 crystals were obtained. This novel method reported here maybe has a guiding significance for the synthesis of manganese oxide materials and other metal oxides using cellulose as template.

1. Introduction

Manganese oxides are important materials due to their potential applications in catalysis, high-density magnetic storage media, ion-exchange, rechargeable batteries, molecular adsorption, and electronics (Armstrong & Bruce, 1996; Bernard, Goff, Thi, & Detorresi, 1993; Chen et al., 2012; Eren, Guney, Eren, & Gumus, 2013; Jothiramalingam, Viswanathan, & Varadarajan, 2005; Shen et al., 1993). More recently, Wang et al. (2013) discovered the manganese oxide micro-supercapacitors with ultra-high areal capacitance. The manganese oxide based composites including manganese oxide/carbon nanofibers (Jung et al., 2012; Kwon et al., 2013) and manganese-oxide-containing mesoporous nitrogen-doped carbon (Tan et al., 2012) have also been reported. The composites from cellulose and manganese oxide could be employed in water purification and removal of heavy metal ion (Maliyekkal, Antony, & Pradeep, 2010a; Maliyekkal, Lisha, & Pradeep, 2010b; Robinson et al., 2013). Maliyekkal et al. (2010b) reported that the Pb(II) adsorption capacity of cellulose/manganese oxide composites was several times higher than commercial manganese oxide and at least twice larger than nanoscale manganese oxide. There have been a few reports on the fabrication of cellulose/manganese oxide composites (Roy, Paice, Archibald, Misra, & Misiak, 1994; Yin, Gao, Wu, Wang, & Lu, 2010). Asiri, Khan, Alamry, Marwani, and Rahman (2013) reported the growth of Mn_3O_4 on cellulose matrix as a solid phase adsorbent for trivalent chromium. Zhou et al. (2011) reported the in-situ synthesis of manganese dioxide nanosheets on cellulose fibers and applied in oxidative decomposition of formaldehyde. In the previous study, a microwave-assisted method was reported for the preparation of cellulose-based composites, which were used as precursor for the synthesis of Mn_2O_3 with similar shape by thermal treatment (Li et al., 2013). Moreover, the microwave-assisted method was also applied for the synthesis of the manganese-containing cellulose nanocomposites using microcrystalline cellulose and $Mn(CH_3COO)_2{\cdot}4H_2O$ in the NaOH/urea aqueous solutions (Ma, Deng, & Yao, 2014). The restrain effect of cellulose treated with NaOH/urea aqueous solutions existed during the procedure of cellulose nanocomposites.

As a green methodology, the sonochemical method is a promising route for the synthesis of functional materials and has been receiving considerable attention thanks to its unusual effects (chemical effect and physical effect) because of acoustic cavitation

* Corresponding author. Tel.: +86 10 62337250; fax: +86 10 62336903.
E-mail address: mg_ma@bjfu.edu.cn (M.-G. Ma).
[1] These authors contributed equally to this work.

http://dx.doi.org/10.1016/j.carbpol.2014.08.098
0144-8617/

Table 1
Preparation of cellulose/Mn_3O_4 composites with four kinds of alkalis.

Samples	Reaction systems
a	MCC (1.00 g) + water (40 mL) + $Mn(CH_3COO)_2{\cdot}4H_2O$ (1.00 g) + urea (1.00 g)
b	MCC (1.00 g) + water (40 mL) + $Mn(CH_3COO)_2{\cdot}4H_2O$ (1.00 g) + HMT (1.00 g)
c	MCC (1.00 g) + water (40 mL) + $Mn(CH_3COO)_2{\cdot}4H_2O$ (1.00 g) + NaOH (1.00 g)
d	MCC (1.00 g) + water (40 mL) + $Mn(CH_3COO)_2{\cdot}4H_2O$ (1.00 g) + KOH (1.00 g)

(Bang & Suslick, 2010; Xu, Zeiger, & Suslick, 2013). More recently, the applications of sonochemical method in the synthesis of inorganic materials have been rapidly growing (Alavi & Morsali, 2010; Askarinejad & Morsali, 2009; Jia, Fan, Zhang, & Qin, 2010). The ultrasound method was applied to synthesize the vaterite spheres by our research group (Fu, Dong, Ma, Li, & Sun, 2013). Recently, Bastami and Entezari (2012) synthesized manganese oxide nanocrystals by ultrasonic bath under external magnetic field. Park et al. (2012) reported the synthesis of graphene oxide/manganese oxide nanocomposites for catalytic glycolysis of poly(ethylene terephthalate) by a sonochemical route. However, to the best of our knowledge, there has been no report on the preparation of cellulose/Mn_3O_4 composites via a sonochemistry method.

In this article, an environmentally-friendly sonochemistry method was applied for the preparation of cellulose/Mn_3O_4 composites using microcrystalline cellulose, $Mn(CH_3COO)_2{\cdot}4H_2O$, and four types of alkalis ($CO(NH_2)_2$, $(CH_2)_6N_4$, NaOH, and KOH) in the deionized water. The thermal stability and the formation mechanism of cellulose-based composites were also investigated.

2. Materials and methods

2.1. Preparation of the cellulose/Mn_3O_4 composites via a sonochemistry method

For the synthesis of target product cellulose/Mn_3O_4 composites, a certain quality of microcrystalline cellulose (MCC) was added into 40 mL deionized water under vigorous stirring. Then, the manganese acetate ($Mn(CH_3COO)_2{\cdot}4H_2O$) and four types of alkalis (urea ($CO(NH_2)_2$), hexamethylenetetramine ($(CH_2)_6N_4$, HMT), NaOH, and KOH) were added into the above solution, respectively. Subsequently, the resulting solution was subjected to sonication (Xin-Zhi, JY92-2D, Ti-horn, 20 kHz, 80 W cm^2) at an ambient condition with a high-density ultrasonic probe immersed directly in the solution. During the ultrasonic irradiation, the reaction solution was kept for 90 min. The detailed experiment parameters were summarized in Table 1. The precipitates were separated from the solution by centrifugation, washed by deionized water and absolute ethanol for several times, then dried in air at 60 °C for further characterization. Afterwards, the obtained products were put into an alumina crucible in a furnace, heated to 600 °C in air with a heating rate of 10 °C min^{-1}, and kept at 600 °C for 3 h.

2.2. Characterization

X-ray powder diffraction (XRD) was performed on a Rigaku D/Max 2200-PC diffractometer with Cu *K*α radiation (λ = 0.15418 nm) and graphite monochromator at ambient temperature. The morphologies of the samples were studied with a scanning electron microscopy (SEM, Hitachi 3400N). All samples were Au coated prior to examination by SEM. Fourier transform infrared (FTIR) spectroscopy was carried out on Thermo Scientific Nicolet iN10 FTIR Microscope (Thermo Nicolet Corporation, Madison, WI, USA), which was equipped with a liquid nitrogen cooled MCT detector. Dried samples were ground and pelletized with BaF_2 and the spectra were recorded in the range of 4000–670 cm^{-1} at 4 cm^{-1} resolution and 64 scans $sample^{-1}$. Thermogravimetric analysis (TGA) and differential thermal analysis (DTA) were taken with a heating rate of 10 °C min^{-1} from room temperature to 600 °C in flowing air with a simultaneous thermal analyzer (Netzsch, STA449F3, Germany).

3. Results and discussion

Using MCC as matrix, the composites were obtained by the addition of $Mn(CH_3COO)_2{\cdot}4H_2O$ and alkali via a sonochemistry method. Four types of alkalis were used in the experimental including urea, HMT, NaOH, and KOH. The XRD patterns of the four obtained samples were recorded for the identification of the products, as shown in Fig. 1. Using urea as alkali, one can see that only the peak of cellulose was observed (marked out by * in Fig. 1a) and no obvious peaks from Mn_2O_3 or Mn_3O_4 or $MnCO_3$ were detected in the XRD pattern of the sample (Fig. 1a). The $MnCO_3$ crystals were obtained using $MnCl_2{\cdot}4H_2O$ and urea using the ultrasonic irradiation method in the literature (Yang, Zhu, Tong, & Wang, 2007). They proposed that urea decomposed homogenously by hydrolysis in the solution according to the following Eqs. (1) and (2), eventually leading to the formation of $MnCO_3$. It is well known that there is a large number of hydroxyl groups exist in the cellulose macromolecular, while the urea hydrates could not be associated directly with cellulose (Cai et al., 2008). The decomposition of urea occurred during the procedure of ultrasonic irradiation. However, no manganese oxides were synthesized in the presence of urea due to the existence of cellulose in this study.

$$CO(NH_2)_2 \rightarrow NH_3 + HNCO \rightarrow NH_4^+ + NCO^- \quad (1)$$

$$NCO^- + OH^- + H_2O \rightarrow NH_3 + CO_3^{2-} \quad (2)$$

Using HMT instead of urea as alkali, weak peaks of Mn_3O_4 appeared (Fig. 1b). In the literature, no manganese oxides were obtained using $Mn(CH_3COO)_2{\cdot}4H_2O$ and HMT in the cellulose matrix via a microwave-assisted method (Li et al., 2013). It was also reported that the well-crystallized Mn_3O_4 was synthesized using $Mn(CH_3COO)_2{\cdot}4H_2O$ and HMT in the deionized water by a microwave-assisted method at 80 °C for 10 min (Yang, Zhu, Tong, Wang, & Cheng, 2006). The temperature of the reaction solution

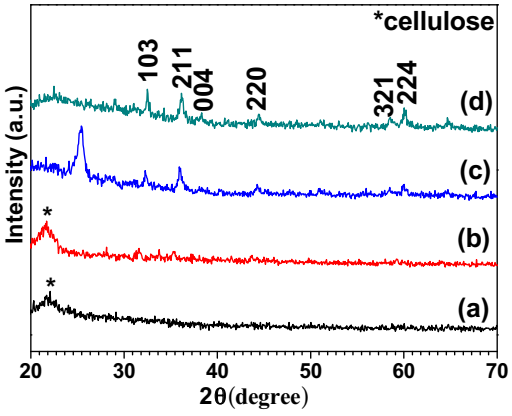

Fig. 1. XRD patterns of the samples prepared by sonochemistry method using different types of alkalis: (a) urea; (b) HMT; (c) NaOH; (d) KOH.

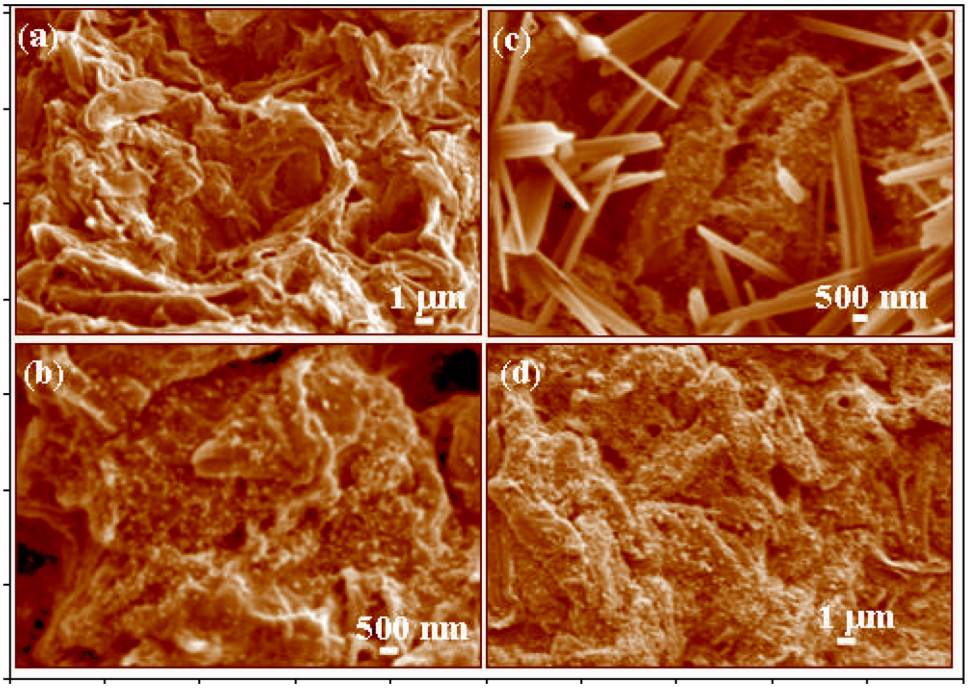

Fig. 2. SEM images of the samples prepared by sonochemistry method using different types of alkalis: (a) urea; (b) HMT; (c) NaOH; (d) KOH.

can run up to around 80 °C during the ultrasonic irradiation process. The formation process of Mn_3O_4 crystals was proposed as the following equations:

$$(CH_2)_6N_4 + 6H_2O \rightarrow 4NH_3 + 6HNCO \quad (3)$$

$$NH_3 + H_2O \rightarrow NH_4^+ + OH^- \quad (4)$$

$$6Mn^{2+} + 12OH^- + O_2 \rightarrow 2Mn_3O_4 + 6H_2O \quad (5)$$

Besides, it is known that $Mn(CH_3COO)_2{\cdot}4H_2O$ can react with HMT in aqueous solution to form Mn_3O_4 at room temperature. Therefore, one can suppose that the existence of cellulose and/or the sonochemistry method decreased the crystallinity of products.

When NaOH was used as alkali, the peaks intensities of Mn_3O_4 increased (Fig. 1c). However, using KOH as alkali, the sample was indexed to well-crystallized Mn_3O_4 with a tetragonal structure (Fig. 1d, JCPDS 24-0734). These results demonstrated that the types of alkalis played an important role in the crystallinity of Mn_3O_4 in cellulose composites. As we all know, the urea and HMT were relatively weak alkalis and KOH and NaOH were relatively strong alkalis. The strong alkalis do a favor for the fabrication of Mn_3O_4 in cellulose composites. There were a large number of hydroxyl groups in the solution, the formation process of Mn_3O_4 maybe explained as follows: First, $Mn(CH_3COO)_2$ reacted with OH^- ions generated white insoluble compound $Mn(OH)_2$, which was easily oxidized by O_2 in air, even the small quantities of O_2 dissolved in water could oxidized it. Subsequently, $Mn(OH)_2$ oxidized by the O_2 in the reaction system generated brown precipitate $MnO(OH)_2$. Then $MnO(OH)_2$ decomposed in the ambient conditions, Mn_3O_4 obtained at last. Under the basic condition, a possible chemical reaction for the synthesis of Mn_3O_4 crystals in the cellulose composites was suggested as follows:

$$Mn(CH_3COO)_2 + 2OH^- \rightarrow 2CH_3COO^- + Mn(OH)_2\downarrow \quad (6)$$

$$2Mn(OH)_2 + O_2 \rightarrow 2MnO(OH)_2\downarrow \quad (7)$$

$$3MnO(OH)_2 \rightarrow Mn_3O_4 + 3H_2O + O_2\uparrow \quad (8)$$

Based on the above analysis results, the cellulose/Mn_3O_4 composites were obtained using $Mn(CH_3COO)_2{\cdot}4H_2O$ and four kinds of alkalis by the sonochemistry method. One can conclude that the types of alkalis played an important role in the crystallinity of Mn_3O_4 in the cellulose composites.

Morphologies and dispersion of Mn_3O_4 in the cellulose matrix are very important for the potential applications of cellulose composites, which were investigated with SEM, as shown in Fig. 2. One can see the Mn_3O_4 crystals grown on the surface of cellulose. Few particles were dispersed on the surface of cellulose using urea as alkali (Fig. 2a). Yet when HMT was selected as additive, the number of Mn_3O_4 particles increased on the surface of cellulose (Fig. 2b). Interestingly, when NaOH was added into the reaction system, the number of the particles ushered in a further increase, what's more, many sheets around 6 μm in length were so conspicuous (Fig. 2c). In the literature, the octahedral Mn_3O_4 nanocrystals were obtained using $Mn(CH_3COO)_2{\cdot}4H_2O$ and NaOH in diluted polyethylene glycol solution at 30 °C (Hao et al., 2011). Both the polyethylene glycol and ultrasonic irradiation are the reasons leading to the difference in the literature. To one's astonishment, the numbers of particles were dramatically increased using KOH as alkali (Fig. 2d), compared with Fig. 2a–c. This SEM results demonstrated that the strong alkalis did a favor for the fabrication of Mn_3O_4 in the cellulose composites.

In addition, one can see that the shape of cellulose was not changed in all four samples and the Mn_3O_4 particles were not mixed with cellulose matrix mechanically. The formation mechanism of cellulose/Mn_3O_4 composites maybe explained as follows: on one hand, Mn_3O_4 crystals maybe absorbed on the surface of cellulose due to the surface electrochemical properties of cellulose that there are many polar groups in the cellulose macromolecules such as hydroxyl groups and uronic acid groups, leading to the negatively charged surface of cellulose in the water. On the other hand, it has been recognized that there are a lot of hydroxyl groups in the molecules, some of them form intra- and intermolecular hydrogen bonds, and others remain free. The cellulose and Mn_3O_4 crystals may be connected with each other through hydroxyl bonds formed from the free hydroxyl groups and Mn_3O_4 crystals, as shown in Scheme 1. Moreover, the ultrasound irradiation had an important role in the synthesis of Mn_3O_4 in the cellulose matrix. In the literature, a H_2O_2-induced oxidation route and a direct

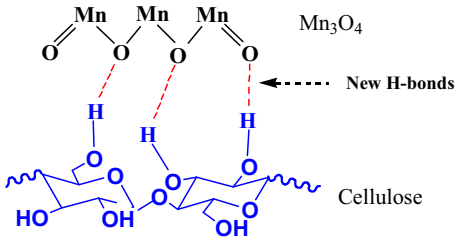

Scheme 1. The possible mechanism between cellulose and Mn_3O_4 crystals.

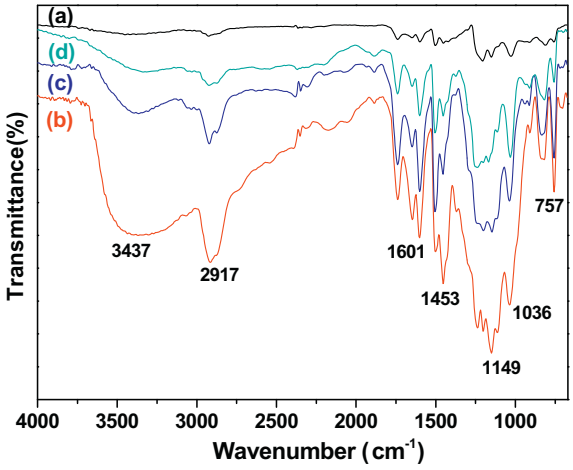

Fig. 3. FTIR spectra of the samples prepared by sonochemistry method using different types of alkalis: (a) urea; (b) HMT; (c) NaOH; (d) KOH.

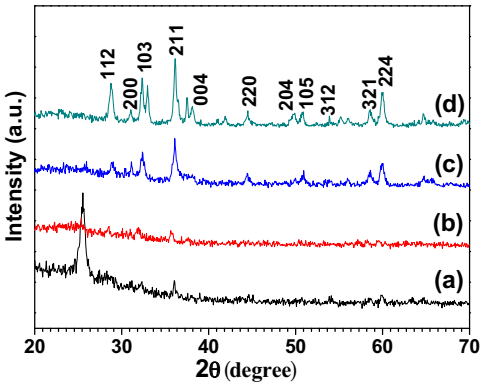

Fig. 5. XRD patterns of the samples by calcination of the cellulose-based composites at 600 °C for 3 h: (a) urea; (b) HMT; (c) NaOH; (d) KOH.

thermal decomposition of hydroxide were suggested for the oxidation of hydroxide to oxide in the thin liquid shell surrounding the cavitation bubble during the ultrasound irradiation process (Choudhury, Choudhary, Sivakumar, & Moholkar, 2013; Goswami, Choudhury, Chakma, & Moholkar, 2013). During the preparation of cellulose/Mn_3O_4 composites, •OH radicals were generated from dissociation of water in the bubble during transient collapse of cavitation bubbles, which induced the synthesis of Mn_3O_4 from manganese hydroxide.

FT-IR spectra of the samples were shown in Fig. 3. The spectra of all samples are similar to each other except Fig. 3a. Among of four FT-IR spectra, the peaks intensities were dramatically weak using urea as alkali (Fig. 3a). The typical characteristic bands of cellulose were observed in all the samples at 3437 cm^{-1} (the stretching vibration of OH), 2917 cm^{-1} (asymmetrically stretching vibration of C—H groups), 1601 cm^{-1} (bending mode of absorbed water in the composites), 1453 cm^{-1} (CH_2 scissoring motion), and 1036 cm^{-1}

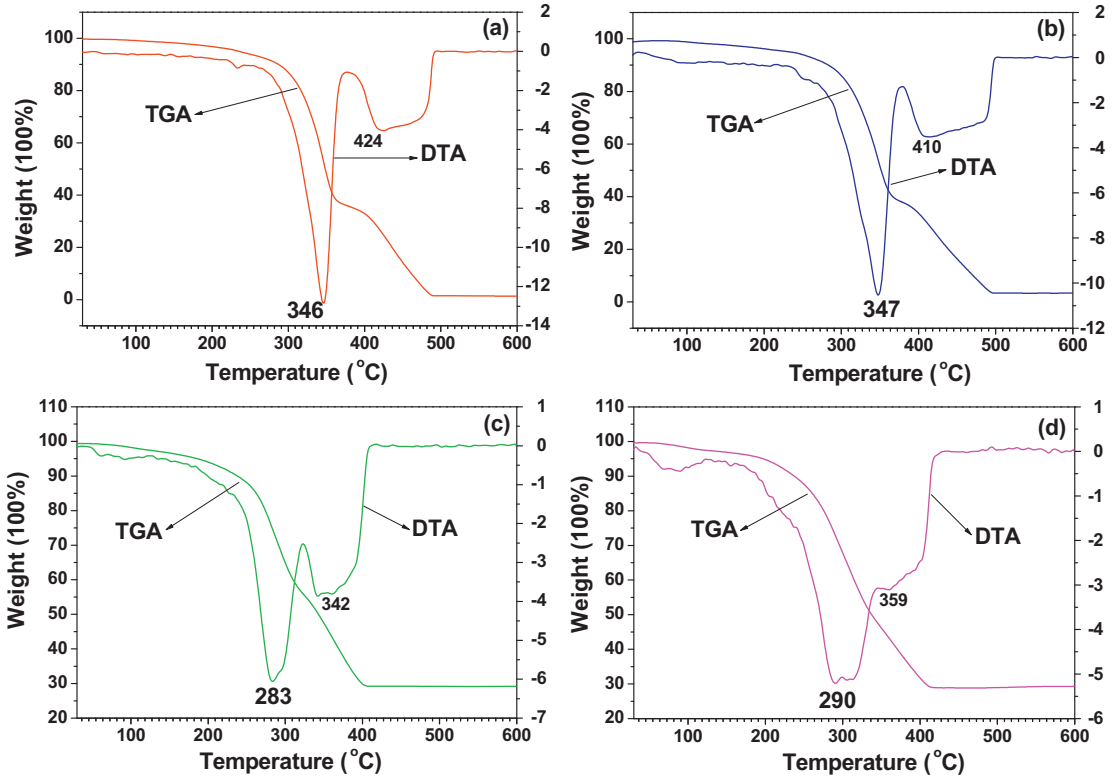

Fig. 4. TGA and DTA curves of the samples prepared by sonochemistry method using (a) urea, (b) HMT, (c) NaOH, and (d) KOH, respectively.

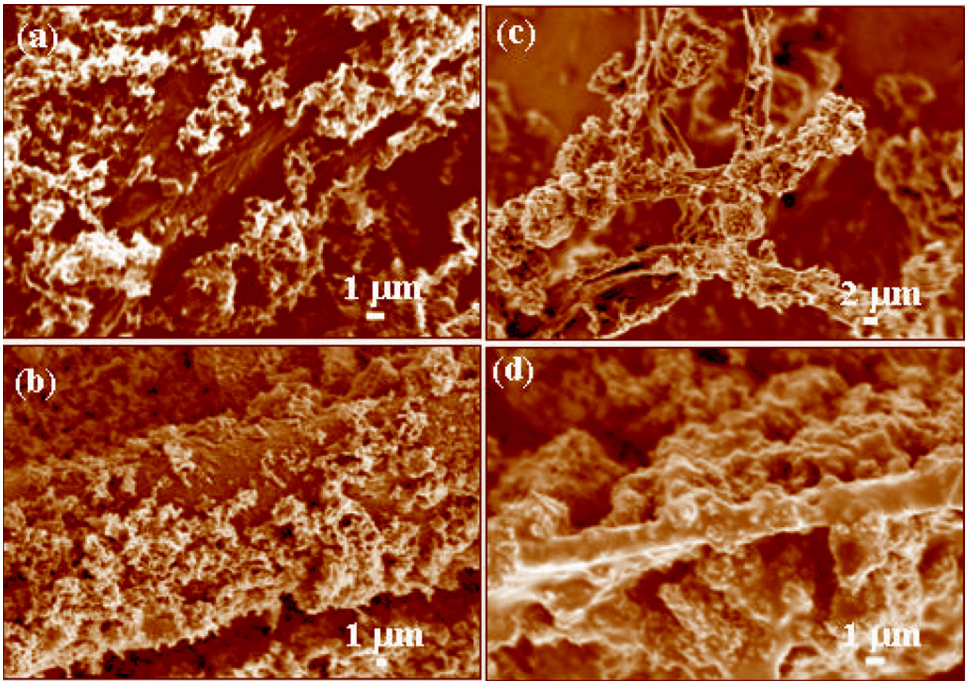

Fig. 6. SEM images of the samples by calcination of the cellulose-based composites at 600 °C for 3 h: (a) urea; (b) HMT; (c) NaOH; (d) KOH.

(C—O—C pyranose ring skeletal vibration of cellulose), which were consistent with that of the pure MCC (Li et al., 2013). Otherwise, the characteristic peaks of Mn—O at 400–650 cm^{-1} were not observed (Gibot and Laffont, 2007). Using HMT as alkali, very strong peaks intensities were observed (Fig. 3b). Using NaOH and KOH as alkali, similar peaks were observed (Fig. 3c and d), compared with Fig. 3b.

The thermal stabilities of the cellulose/Mn_3O_4 composites were investigated with TGA and DTA (Fig. 4). The total weight losses of the four composites were measured to be 98.5%, 96.7%, 70.8%, and 71.4%. That is to say, the contents of Mn_3O_4 were 1.5%, 3.3%, 29.2%, and 28.6%, respectively. The percent of Mn_3O_4 was very low in the cellulose composites using urea and HMT as alkalis (Fig. 4a and b); meanwhile, the percents of Mn_3O_4 were dramatically increased from 1.5%/3.3% to 29.2%/28.6% in the cellulose composites using NaOH and KOH as alkalis (Fig. 4c and d). These results demonstrated that the types of alkalis played an important role in the synthesis of Mn_3O_4. All TGA curves displayed two stages of weight losses, which were assigned to the thermal degradation and complete decomposition of cellulose in composites. What's more, the ending temperatures were 487, 495, 404, and 416 °C for the samples prepared using urea, HMT, NaOH, and KOH, respectively. The ending temperatures of the composites synthesized using NaOH and KOH obvious decreased, compared with using urea and HMT. It was supposed that the decreasing ending temperatures maybe due to the interaction between Mn_3O_4 and cellulose in composites. These results indicated that the addition of Mn_3O_4 decreased the thermal stability of cellulose in composites. Furthermore, two endothermic peaks were located at 346/424, 347/410, 283/342, and 290/359 °C in the DTA curves for the fours samples, which fitted well with those of weight losses in the TGA curves. Two endothermic peaks of four samples displayed similar phenomenon. Based on the results of TGA and DTA, one can conclude that the cellulose/Mn_3O_4 composites provided the possibility for the improvement of thermal stabilities due to the interaction between the counterparts, compared with the individual components.

Based on the results of TGA and DTA, 600 °C was chosen as the calcination temperature for the complete decomposition of cellulose/Mn_3O_4 composites. After the calcination of the as-prepared cellulose composites at 600 °C for 3 h in air, the Mn_3O_4 crystals were obtained. The XRD patterns of the as-obtained Mn_3O_4 samples are shown in Fig. 5. One can see that the peak of cellulose disappeared. The XRD patterns displayed weak peaks of Mn_3O_4 using urea and HMT as alkalis (Fig. 5a and b). On the contrary, the peaks intensities of Mn_3O_4 were obvious increased using NaOH and KOH as alkalis (Fig. 5c and d). The phase of Mn_3O_4 did not change after the calcination but the peaks intensities increased, compared with Fig. 1, demonstrating that the calcination favored the increasing crystallinity of inorganic crystals. Moreover, the cellulose decomposed by calcination, favoring the increasing peaks intensities of Mn_3O_4. Fig. 6 shows the morphologies of Mn_3O_4 samples, which were prepared by thermal treatment using cellulose/Mn_3O_4 composites at 600 °C for 3 h in air. The shapes of Mn_3O_4 crystals were sustained after the calcinations except the sheets disappeared. In comparison with the cellulose/Mn_3O_4 composites, the irregular particles were observed after calcination using urea and HMT as alkalis (Fig. 6a and b). The fiber-like shape maybe assign to the carbon by the decomposition of MCC. Using NaOH and KOH as alkalis, Mn_3O_4 particles were still obvious observed (Fig. 6c and d). The calcination did not improve the dispersion of Mn_3O_4 particles.

4. Conclusions

In summary, compare study cellulose/Mn_3O_4 composites were conducted among four types of alkalis by the sonochemistry method. The Mn_3O_4 crystals were obtained after the thermal decomposition of the cellulose/Mn_3O_4 composites at 600 °C for 3 h. Experimental results demonstrated that the types of alkalis played an important role in the phase, shape, dispersion, and thermal stability of cellulose/Mn_3O_4 composites. This novel method provides a new strategy for the synthesis of manganese oxide materials using cellulose as template. This method reported here may be has a guiding significance for the synthesis of other metal oxides particles.

Acknowledgments

Financial supports from Beijing Nova Program (Z121103002512030), the Program for New Century Excellent Talents in University (NCET-11-0586) and National Natural Science Foundation of China (51302264) is gratefully acknowledged.

References

Alavi, M. A., & Morsali, A. (2010). Syntheses and characterization of $Mg(OH)_2$ and MgO nanostructures by ultrasonic method. *Ultrasonics Sonochemistry*, *17*, 441–446.

Armstrong, A. R., & Bruce, P. G. (1996). Synthesis of layered $LiMnO_2$ as an electrode for rechargeable lithium batteries. *Nature*, *381*, 499–500.

Asiri, A. M., Khan, S. B., Alamry, K. A., Marwani, H. M., & Rahman, M. M. (2013). Growth of Mn_3O_4 on cellulose matrix: Nanohybrid as a solid phase adsorbent for trivalent chromium. *Applied Surface Science*, *270*, 539–544.

Askarinejad, A., & Morsali, A. (2009). Direct ultrasonic-assisted synthesis of sphere-like nanocrystals of spinel Co_3O_4 and Mn_3O_4. *Ultrasonics Sonochemistry*, *16*, 124–131.

Bang, J. H., & Suslick, K. S. (2010). Applications of ultrasound to the synthesis of nanostructured materials. *Advanced Materials*, *22*, 1039–1059.

Bastami, T. R., & Entezari, M. H. (2012). Synthesis of manganese oxide nanocrystal by ultrasonic bath: Effect of external magnetic field. *Ultrasonics Sonochemistry*, *19*, 830–840.

Bernard, M. C., Goff, A. H. L., Thi, B. V., & Detorresi, S. C. (1993). Electrochromic reactions in manganese oxides. *Journal of Electrochemical Society*, *140*, 3065–3070.

Cai, J., Zhang, L. N., Liu, S. L., Xi, X. J., Chen, X. M., Chu, B. J. M., et al. (2008). Dynamic self-assembly induced rapid dissolution of cellulose at low temperatures. *Macromolecules*, *41*, 9345–9351.

Chen, Z. W., Jiao, Z., Pan, D. Y., Li, Z., Wu, M. H., Shek, C. H., et al. (2012). Recent advances in manganese oxide nanocrystals: Fabrication, characterization, and microstructure. *Chemical Reviews*, *112*, 3833–3855.

Choudhury, H. A., Choudhary, A., Sivakumar, M., & Moholkar, V. S. (2013). Mechanistic investigation of the sonochemical synthesis of zinc ferrite. *Ultrasonics Sonochemistry*, *20*, 294–302.

Eren, E., Guney, M., Eren, B., & Gumus, H. (2013). Performance of layered birnessite-type manganese oxide in the thermal-catalytic degradation of polyamide 6. *Applied Catalysis B: Environmental*, *132*, 370–378.

Fu, L. H., Dong, Y. Y., Ma, M. G., Li, S. M., & Sun, R. C. (2013). Compare study $CaCO_3$ crystals on the cellulose substrate by microwave-assisted method and ultrasound agitation method. *Ultrasonics Sonochemistry*, *20*, 839–845.

Gibot, P., & Laffont, L. (2007). Hydrophilic and hydrophobic nano-sized Mn_3O_4 particles. *Journal of Solid State Chemistry*, *180*, 695–701.

Goswami, P. P., Choudhury, H. A., Chakma, S., & Moholkar, V. S. (2013). Sonochemical synthesis and characterization of manganese ferrite nanoparticles. *Industrial & Engineering Chemistry Research*, *52*, 17848–17855.

Hao, X. L., Zhao, J. Z., Li, Y. L., Zhao, Y., Ma, D. C., & Li, L. Z. (2011). Mild aqueous synthesis of octahedral Mn_3O_4 nanocrystals with varied oxidation states. *Colloids and Surfaces A: Physicochemical and Engineering Aspects*, *374*, 42–47.

Jia, X. H., Fan, H. Q., Zhang, F. Q., & Qin, L. (2010). Using sonochemistry for the fabrication of hollow ZnO microspheres. *Ultrasonics Sonochemistry*, *17*, 284–287.

Jothiramalingam, R., Viswanathan, B., & Varadarajan, T. K. (2005). Preparation, characterization and catalytic properties of cerium incorporated porous manganese oxide OMS-2 catalysts. *Catalysis Communications*, *6*, 41–45.

Jung, K. N., Lee, J. I., Yoon, S., Yeon, S. H., Chang, W., Shin, K. H., et al. (2012). Manganese oxide/carbon composite nanofibers: Electrospinning preparation and application as a bi-functional cathode for rechargeable lithium–oxygen batteries. *Journal Materials Chemistry*, *22*, 21845–21848.

Kwon, O. S., Kim, T., Lee, J. S., Park, S. J., Park, H. W., Kang, M., et al. (2013). Fabrication of graphene sheets intercalated with manganese oxide/carbon nanofibers: Toward high-capacity energy storage. *Small*, *9*, 248–254.

Li, S. M., Wang, Y. L., Ma, M. G., Zhu, J. F., Sun, R. C., & Xu, F. (2013). Microwave-assisted method for the synthesis of cellulose-based composites and their thermal transformation to Mn_2O_3. *Industrial Crops and Products*, *43*, 751–756.

Ma, M. G., Deng, F., & Yao, K. (2014). Manganese-containing cellulose nanocomposites: Microwave synthesis, characterization, and the restrain effect of cellulose. *Carbohydrate Polymers*, *111*, 230–235.

Maliyekkal, S. M., Antony, A. K. R., & Pradeep, T. (2010). High yield combustion synthesis of nanomagnesia and its application for fluoride removal. *Science of the Total Environment*, *408*, 2273–2282.

Maliyekkal, S. M., Lisha, K. P., & Pradeep, T. (2010). A novel cellulose-manganese oxide hybrid material by in situ soft chemical synthesis and its application for the removal of Pb(II) from water. *Journal of Hazardous Materials*, *181*, 986–995.

Park, G., Bartolome, L., Lee, K. G., Lee, S. J., Kim, D. H., & Park, T. J. (2012). One-step sonochemical synthesis of a graphene oxide–manganese oxide nanocomposite for catalytic glycolysis of poly(ethylene terephthalate). *Nanoscale*, *4*, 3879–3885.

Robinson, D. M., Go, Y. B., Mui, M., Gardner, G., Zhang, Z. J., Mastrogiovanni, D., et al. (2013). Photochemical water oxidation by crystalline polymorphs of manganese oxides: Structural requirements for catalysis. *Journal of the American Chemical Society*, *135*, 3494–3501.

Roy, B. P., Paice, M. G., Archibald, F. S., Misra, S. K., & Misiak, L. E. (1994). Creation of metal-complexing agents, reduction of manganese dioxide, and promotion of manganese peroxidase-mediated Mn(III) production by cellobiose:quinone oxidoreductase from trametes versicolor. *The Journal of Biological Chemistry*, *269*, 19745–19750.

Shen, Y. F., Zerger, R. P., Deguzman, R. N., Suib, S. L., Mccurdy, L., Potter, D. I., et al. (1993). Manganese oxide octahedral molecular sieves: Preparation, characterization, and applications. *Science*, *260*, 511–515.

Tan, Y. M., Xu, C. F., Chen, G. X., Fang, X. L., Zheng, N. F., & Xie, Q. J. (2012). Facile synthesis of manganese-oxide-containing mesoporous nitrogen-doped carbon for efficient oxygen reduction. *Advanced Functional Materials*, *22*, 4584–4591.

Wang, X., Myers, B. D., Yan, J., Shekhawat, G., Dravid, V., & Lee, P. S. (2013). Manganese oxide micro-supercapacitors with ultra-high areal capacitance. *Nanoscale*, *5*, 4119–4122.

Xu, H. X., Zeiger, B. W., & Suslick, K. S. (2013). Sonochemical synthesis of nanomaterials. *Chemical Society Reviews*, *42*, 2555–2567.

Yang, L. X., Zhu, Y. J., Tong, H., Wang, W. W., & Cheng, G. F. (2006). Low temperature synthesis of Mn_3O_4 polyhedral nanocrystals and magnetic study. *Journal of Solid State Chemistry*, *179*, 1225–1229.

Yang, L. X., Zhu, Y. J., Tong, H., & Wang, W. W. (2007). Submicrocubes and highly oriented assemblies of $MnCO_3$ synthesized by ultrasound agitation method and their thermal transformation to nanoporous Mn_2O_3. *Ultrasonics Sonochemistry*, *14*, 259–265.

Yin, J. Z., Gao, F., Wu, Y. F., Wang, J. J., & Lu, Q. Y. (2010). Synthesis of Mn_3O_4 octahedrons and other manganese-based nanostructures through a simple and green route. *CrystEngComm*, *12*, 3401–3403.

Zhou, L., He, J. H., Zhang, J., He, Z. C., Hu, Y. C., Zhang, C. B., et al. (2011). Facile in-situ synthesis of manganese dioxide nanosheets on cellulose fibers and their application in oxidative decomposition of formaldehyde. *The Journal of Physical Chemistry C*, *115*, 16873–16878.